

# Dissociation Kinetics of Methane Hydrate in Frozen Rocks under Decreasing External Pressure: Mathematical and Experimental Modeling

M. M. Ramazanov<sup>a,b,\*</sup>, N. S. Bulgakova<sup>a,c</sup>, Academician L. I. Lobkovsky<sup>d,e</sup>, E. M. Chuvilin<sup>e,f</sup>,  
D. A. Davletshina<sup>b,e,f</sup>, and N. E. Shakhova<sup>b,e,g</sup>

Received December 4, 2023; revised February 14, 2024; accepted February 20, 2024

**Abstract**—The results of mathematical and experimental modeling of dissociation of pore methane hydrate in ice- and gas-bearing sediments with a decrease in the external pressure below equilibrium are presented. The described model of pore gas hydrate dissociation at negative temperatures, along with the experiment, makes it possible to calculate the kinetics of this process. A comparative analysis of the results is conducted. The proposed mathematical model confirms the trend of decreasing hydrate saturation of frozen soil in the form of  $S_h \sim A\tau^{-n}$  obtained previously in experiments. These experiments have made it possible to calculate the coefficients  $A$  and  $n$ , while the mathematical modeling shows how these coefficients depend on the problem parameters. The theoretically estimated properties of the coefficient fully confirm the experimental data. The results of experimental and mathematical modeling have implications for key factors that determine the self-preservation of pore methane hydrates in frozen sediments.

**Keywords:** permafrost, methane hydrate, porous media, dissociation, self-preservation, mathematical modeling, experimental modeling

**DOI:** 10.1134/S1028334X24601391

## INTRODUCTION

Today gas hydrates are a promising alternative source of hydrocarbons on the one hand and a source of hazards associated with technological and environmental risks on the other hand. It is known that the possibility for the existence of gas hydrate deposits in permafrost areas is explained by the emergence of the necessary conditions for their formation and the pres-

ence of significant volumes of gas accumulations. The occurrence of such favorable conditions within permafrost strata is related to the long-term fluctuations in the surface temperature of the Earth and long-term cooling of lithospheric rocks. Gas accumulations existing in the upper horizons of the lithosphere under such conditions may penetrate the gas hydrate stability zone (GHSZ), which leads to the conversion of a part of the gas into a gas hydrate state [1–3].

Favorable conditions for the formation of gas hydrates in cryolithozone rocks may also be created by a baric factor associated with the formation of an ice sheet on the permafrost surface or with transgressions of Arctic seas [4]. Additionally, this could be related to the cryogenic concentration of gas fluids and their accumulation in horizons with good reservoir properties during the freezing of gas-bearing rocks, as well as to the generation of excess pressure required for the transformation of gas into gas hydrates [3, 5, 6].

In the areas with permafrost rocks, gas hydrates can be found both beneath the permafrost (the most extensively studied at the present time) and within the permafrost at negative temperatures, the actual data on their occurrence mainly have an indirect character. Furthermore, there is evidence about the possible existence of metastable gas hydrates within permafrost strata above the modern roof of the gas hydrate stabil-

<sup>a</sup>*Institute for Problems of Geothermy and Renewable Energy, Branch of the Joint Institute for High Temperatures, Russian Academy of Sciences, Makhachkala, 367030 Russia*

<sup>b</sup>*Sadovskii Institute of Geosphere Dynamics, Moscow, 119334 Russia*

<sup>c</sup>*Dagestan State University of National Economy, Makhachkala, 367008 Russia*

<sup>d</sup>*Shirshov Institute of Oceanology, Russian Academy of Sciences, Moscow, 117997 Russia*

<sup>e</sup>*Science Department, Tomsk State University, Tomsk, 634050 Russia*

<sup>f</sup>*Center for Petroleum Science and Engineering, Skolkovo Institute of Science and Technology (Skoltech), Skolkovo Innovation Center, Moscow, 121205 Russia*

<sup>g</sup>*Il'ichev Pacific Oceanological Institute, Far East Branch, Russian Academy of Sciences, Vladivostok, 690041 Russia*

\*e-mail: mukamay-ipg@mail.ru

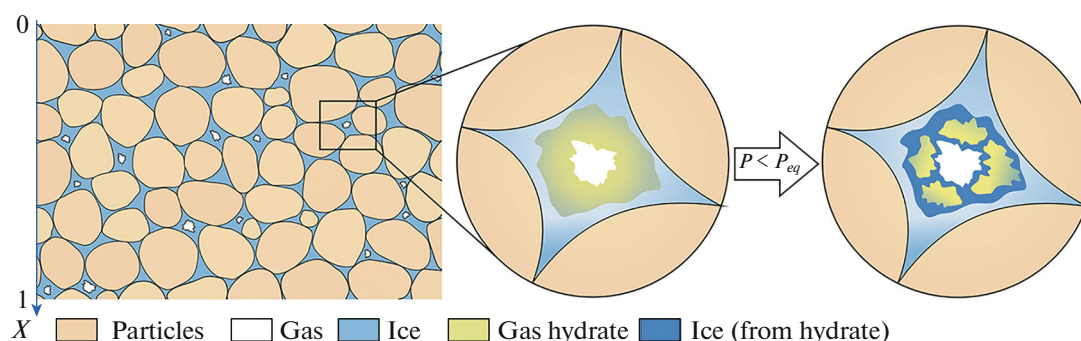


**Fig. 1.** Schematic model of the pore space of frozen gas hydrate-bearing sandy soil under equilibrium and non-equilibrium conditions.

ity zone at depths down to 150–200 m. Their formation is associated with paleo-GHSZ, and their preservation is determined by the geological manifestation of the self-preservation effect of gas hydrates in permafrost rocks [7, 8]. It is the metastable gas hydrates that are extremely sensitive to various external effects, which make these formations a source of geological risk in the exploration and exploitation of oil and gas fields in the Arctic region.

In this regard, in recent decades, researchers have paid considerable attention to the experimental study of decomposition processes of gas hydrates in the pore space of gas-saturated ice-containing rocks [6, 9–11]. However, the analysis of the published data showed that today there are relatively few works on the theoretical study of the dissociation and self-preservation processes of gas hydrates in the pore space at negative temperatures [12–18].

Despite the presence of experimental and theoretical works devoted to the study of decomposition of pore hydrate formations, the integration of two research areas and the simultaneous application of

experimental and mathematical modeling to study the kinetics and self-preservation of gas hydrates in permafrost rocks appear to be quite urgent.

### MATHEMATICAL STUDY

**Problem statement.** We assume that a horizontal layer of frozen dispersed rock with thickness contains ice, gas, and gas hydrates in the pore space, initially in thermodynamic equilibrium at a given negative Celsius temperature  $T_0$  and the corresponding equilibrium pressure  $p_0 = p_0(T_0)$  (Fig. 1). At some instant, the pressure above the layer drops below the three-phase equilibrium point to the value  $p^0 < p_0$  and the gas hydrate begins to decompose. In this process, part of the pore inclusions of the gas hydrate may completely decompose, while another part undergoes only partial dissociation, to some extent passing to a metastable state due to the formation of an ice crust as a result of manifestation of the self-preservation effect. Whether these gas hydrate inclusions will remain or dissociate slowly will depend on the ability of the ice crust to withstand the pressure difference  $p_0 - p^0$  at the first significantly non-stationary stage [18]. Thus, the greater the decrease in external pressure, the less preservation of gas hydrate inclusions is expected with time due to the self-preservation effect. There arises a need to assess the kinetics of this process at the second quasi-stationary stage using theoretical and experimental methods and to conduct their comparative analysis.

Later on, for clarity, we will consider a simplified model structure of the gas hydrate. Namely, we assume that the pore gas hydrate inclusions can be represented as a set of granules of spherical configuration (Fig. 2) [13, 18].

The first outer layer of the granule consists of a poorly permeable ice crust, the thickness of which increases inward during the decomposition of the granule; the second layer is a thin gas layer, the thickness of which is not considered. It is assumed that the

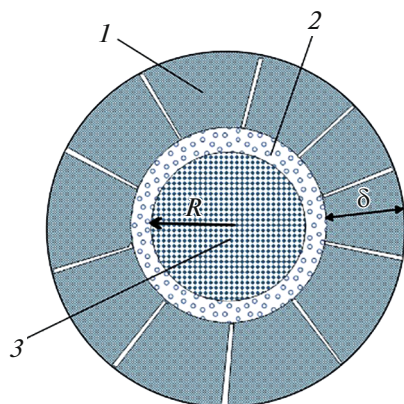


**Fig. 2.** Three-layer scheme of gas hydrate granule dissociation: (1) ice crust with thickness  $\delta$ ; (2) thin layer of methane formed during gas hydrate decomposition; (3) undissolved methane hydrate, the thermodynamic conditions of which correspond to the steady state.

gas pressure in this layer is equal to the equilibrium pressure of the gas hydrate at the given temperature  $p_0$ ; the third layer is the undecomposed gas hydrate (the core of the gas hydrate granule). During the decomposition of the granule, the radius of its core decreases; i.e., the phase transition front moves towards the center of the core. In this process, due to the pressure difference  $p_0 - p$ , the released gas filters through the pores and microcracks of the ice layer into the porous medium saturated with ice, gas, and gas hydrate and, due to the pressure gradient in this medium, is unloaded through the upper boundary of the layer (Fig. 1).

We emphasize that the scheme in Fig. 2 may vary. Specifically, layer 2 may be absent and free gas fills the micropores and microcracks in layer 1 [13]. There may also be a case in which there are no connected micro- and mesopores and cracks, and the gas transits from the hydrate phase to the free phase by gas diffusion through the ice. We note that the solution obtained below is applicable in all cases, and the third case differs only in the expression of the coefficient  $a_2$  in formula (11). In this case, the expression  $k_2 \bar{p} / \mu$  in the coefficient  $a_2$  should be replaced with the gas diffusion coefficient in ice  $D$ .

Finally, we consider the set of all granules in a unit volume of the medium in the model as one effective granule, where the ice crust layer is equal to the effective sum of the ice crust layers of individual granules, the core radius of the effective granule is equal to the effective sum of the radii of all microgranules, and so on.

**Mathematical model.** Let the  $x$ -axis be directed downwards, and we choose the coordinate system as shown in Fig. 1. The equations describing the process of gas hydrate degradation within the problem statement can be written as

$$v = -\frac{k_1}{\mu} \frac{\partial p}{\partial x}, \quad (1)$$

$$\phi_g \frac{\partial \rho_g}{\partial t} + \rho_g \frac{\partial \phi_g}{\partial t} + \frac{\partial}{\partial x} (\rho_g v) = \frac{k_2 \rho_g}{\mu} \frac{q(p_0, p^0, p_\infty, p)}{\delta^2(t)}, \quad (2)$$

$$\delta(t) = R(0) - R(t) = \sqrt{\gamma t},$$

$$\rho_g = \frac{p}{R_g T_0}. \quad (3)$$

Here,  $v$  is the gas filtration velocity;  $t$  is the time;  $\phi_g$  is the fraction of gas saturated reservoir pores;  $k_1$  and  $k_2$  are the effective permeabilities of the reservoir as a whole and the ice crust in the gas hydrate granules;  $\rho_g$  is the gas density;  $p$  is the gas pressure;  $T_0$  is the assigned gas temperature;  $R_g$  is the specific gas constant of methane;  $\mu$  is the gas viscosity;  $\delta(t)$  is the ice crust thickness in the effective gas hydrate granule;  $R(0)$  and  $R(t)$  are the outer and inner radii of the ice

crust;  $\gamma$  is the effective coefficient characterizing the phase transition front movement into the core of the gas hydrate granule;  $q(p_0, p^0, p_\infty, p)$  is the function determining the pressure dependence of the intensity of gas hydrate decomposition;  $p_\infty(t)$  is the pressure at the bottom boundary of the reservoir determined from the solution of the problem.

In system (1)–(3), the first equation is Darcy's law for gas filtration in the reservoir, the second is the gas mass balance equation, and the third is the equation of the gas state. Note that the last term in Eq. (2) is a source of gas related to gas hydrate decomposition in the granules.

Next, we replace the condition at the bottom boundary of the reservoir with the condition at infinity, which allows finding an analytical solution to the problem and will not lead to qualitative or quantitative distortions of the results.

We rewrite (1)–(3) together with the boundary and initial conditions as

$$\phi \frac{\partial p}{\partial t} = \frac{\partial}{\partial x} \left( \frac{k_1 p}{\mu} \frac{\partial p}{\partial x} \right) + \frac{k_2 p}{\mu \gamma} \frac{q(p_0, p^0, p_\infty, p)}{t}, \quad (4)$$

$$\phi = \phi_g + p \frac{\partial \phi_g}{\partial p},$$

$$p(0, t) = p^0, \quad \frac{\partial p}{\partial x}(\infty, t) = 0, \quad (5)$$

$$p(x, 0) = p_0. \quad (6)$$

We further in (4) refer  $\phi$  to some average pressure and consider it to be a constant.

We define the function  $q(p_0, p^0, p_\infty, p)$ . In (4)–(6), as a result of gas hydrate degradation, the pressure at an arbitrary final point should tend to the external pressure  $p^0$ ; therefore, we assume that

$$q(p_0, p^0, p_\infty, p) \rightarrow 0, \quad \text{at } p \rightarrow p^0. \quad (7)$$

At infinity, the condition should satisfy

$$q(p_0, p^0, p_\infty, p) \rightarrow p_0 - p_\infty, \quad \text{at } p \rightarrow p_\infty. \quad (8)$$

The simplest function satisfying conditions (7)–(8) takes on the form

$$q(p_0, p^0, p_\infty, p) = \frac{p_0 - p_\infty}{p_\infty - p^0} (p - p^0). \quad (9)$$

We introduce the scales

$$[t] = t_0, \quad [x] = l, \quad [p] = p^0. \quad (10)$$

Denoting the dimensionless pressure by  $\sigma$ , we have

$$\frac{\partial \sigma}{\partial t} = \frac{k_1 p^0 t_0}{\phi \mu l^2} \frac{\partial}{\partial x} \left( \sigma \frac{\partial \sigma}{\partial x} \right) + \frac{k_2 p^0 \sigma \sigma_0 - \sigma_\infty \sigma - 1}{\phi \mu \gamma \sigma_\infty - 1} \frac{1}{t},$$

$$\sigma = \frac{p}{p^0}, \quad \sigma_0 = \frac{p_0}{p^0}, \quad \sigma_\infty = \frac{p_\infty}{p^0}.$$

Linearizing this equation using some average pressure  $\bar{p}$ , we obtain

$$\frac{\partial \sigma}{\partial t} = \frac{k_1 \bar{p} t_0}{\phi \mu l^2} \frac{\partial^2 \sigma}{\partial x^2} + \frac{k_2 \bar{p} \sigma_0 - \sigma_\infty \sigma - 1}{\phi \mu \gamma \sigma_\infty - 1} \frac{1}{t}.$$

Or, together with boundary conditions

$$\frac{\partial \sigma}{\partial t} = a_1 \frac{\partial^2 \sigma}{\partial x^2} + a_2 \frac{\sigma_0 - \sigma_\infty \sigma - 1}{\sigma_\infty - 1} \frac{1}{t}, \quad a_1 = \frac{k_1 \bar{p} t_0}{\mu \phi l^2}, \quad (11)$$

$$a_2 = \frac{k_2 \bar{p}}{\gamma \mu \phi}, \quad \sigma(0, t) = 1, \quad \frac{\partial \sigma}{\partial x}(\infty, t) = 0,$$

$$\sigma = \frac{p}{p^0}, \quad \sigma_0 = \frac{p_0}{p^0}, \quad \sigma_\infty = \frac{p_\infty}{p^0}. \quad (12)$$

As we already mentioned in the Introduction, in the case of the absence of connected micro- and mesopores and cracks in the ice crust, and gas transits from the hydrate phase to the free phase by gas diffusion through ice, the coefficient  $a_2$  in (11) is written as  $a_2 = D/(\gamma \phi)$ , where  $D$  is the coefficient of gas diffusion through the ice.

We find the dimensionless pressure at infinity  $\sigma_\infty(t)$ , which, due to the second Eq. (5), depends only on time. In this case, we have the equation from (11)

$$\frac{d\sigma_\infty}{dt} = a_2 \frac{\sigma_0 - \sigma_\infty}{t}.$$

By integrating this equation, we have

$$\sigma_\infty(t) = \sigma_0 - C_0 t^{-a_2}. \quad (13)$$

Here, constant  $C_0$  is related to the initial hydrate saturation of the reservoir.

Now we need to find the dimensionless pressure  $\sigma$  to satisfy (11).

We search for the solution to this problem in the form

$$\sigma = 1 + (\sigma_0 - 1 - C_0 t^{-a_2}) f(\xi), \quad \xi = \frac{x}{\sqrt{t}}, \quad (14)$$

where  $f(\xi)$  is the function sought.

Substituting (14) into (11), we have

$$-\frac{\xi}{2} \frac{df}{d\xi} = a_1 \frac{d^2 f}{d\xi^2}, \quad (15)$$

$$f(0) = 0, \quad f(\infty) = 1.$$

The solution (15) has the form

$$f = \operatorname{erf} \left( \frac{\xi}{\sqrt{2a_1}} \right). \quad (16)$$

Thus, we obtain the following distribution of dimensionless pressure in the gas

$$\sigma = 1 + (\sigma_0 - 1 - C_0 t^{-a_2}) \operatorname{erf} \left( \frac{\xi}{\sqrt{2a_1}} \right), \quad \xi = \frac{x}{\sqrt{t}}. \quad (17)$$

The rate of change in residual hydrate saturation is expressed as

$$\frac{R_g T_0 (1 - \gamma_i) \rho_h}{p^0} \frac{\partial S_h}{\partial t} = -a_2 \frac{\sigma_0 - \sigma_\infty \sigma - 1}{\sigma_\infty - 1} \frac{1}{t} \quad (18)$$

$$= -a_2 C_0 t^{-a_2-1} \operatorname{erf} \left( \frac{\xi}{\sqrt{2a_1}} \right).$$

Here,  $S_h$  is the residual hydrate saturation.  $\rho_h$  is the gas hydrate density.  $\gamma_i$  is the mass fraction of water (ice) in the gas hydrate, and  $(1 - \gamma_i)$  is the mass fraction of gas in the gas hydrate.

Formula (18) means that the intensity of the free gas source in (11) is determined by the rate of decrease in the mass of gas in the hydrate state.

By integrating (18) in the first approximation, we obtain

$$S_h = \frac{p^0}{R_g T_0 (1 - \gamma_i) \rho_h} C_0 t^{-a_2} \operatorname{erf} \left( \frac{\xi}{\sqrt{2a_1}} \right), \quad \xi = \frac{x}{\sqrt{t}}. \quad (19)$$

Equality (19) gives mixed kinetics. In this case, the coefficient  $a_2$  is responsible for its own kinetics, while the coefficient  $a_1$  relates to the gas filtration kinetics.

## EXPERIMENTAL STUDY

For experimental modeling of the dissociation kinetics for methane hydrate inclusion in frozen rocks at a decreasing external pressure, we used a special setup that allowed for artificial hydrate saturation of soil media under specified thermobaric conditions over a wide range of temperatures and pressures. Sand sampled from gas-bearing horizons of frozen rocks in the northern part of Western Siberia was used as the study object. The predominant fraction in the soil was sand 0.25–0.1 mm in size (~60.5%), with a dust fraction (0.05–0.001 mm) comprising about 3.7%. Particles <0.001 mm did not exceed 0.7%. Quartz was the predominant mineral. The sand was characterized by low salinity ( $Z$ , no greater than 0.05%).

*Experimental setup.* The setup (Top Industrie, France) comprised a pressure chamber with a volume of 570 cm<sup>3</sup> (internal diameter of 70 mm, height of 150 mm) and an operating pressure up to 15 MPa. The setup was equipped with a liquid cryostat (JULABO, Germany), enabling setting working temperatures from –20°C to +40°C. The temperature in the pressure chamber was maintained with an accuracy of 0.1°C, while the pressure was monitored with an accuracy of 0.1 MPa [19]. The pressure chamber was a sealed steel cylinder with a thermal insulating coat and

inlet pipes for the inflow of cooling liquid. A soil sample with a diameter of 4.6 cm and a height of  $\approx 10$  cm contained in a plastic container is placed inside the pressure chamber. The lid of the pressure chamber has two temperature sensors, 40 and 60 mm long and 1 mm in diameter, as well as fittings for gas pressure supply and measurement.

**Experimental procedure.** The methodology for obtaining a hydrate-saturated medium involved preparing a soil sample with a specified moisture content, placing it in the pressure chamber's core holder, freezing it to  $-6\ldots-8^\circ\text{C}$ , feeding methane to a pressure higher than the equilibrium pressure for hydrate formation (6–8 MPa), and saturation of the frozen sample with methane hydrate during several days at a fixed negative temperature. Additional freezing–thawing cycles (from  $-6\ldots-8^\circ\text{C}$  to  $+2^\circ\text{C}$ ) were used to increase the hydrate content in the samples. Upon ice melting, the process of hydrate formation in the pore space intensified due to the creation of additional gas–water contacts [19]. After hydrate accumulation was completed, the frozen hydrate-saturated sample was subjected to non-equilibrium conditions at a fixed negative temperature ( $\sim -6^\circ\text{C}$ ). To do this, the pressure in the pressure chamber with the sample was reduced to 0.1 MPa [6, 11, 19].

As a result of analysis of the changes in thermobaric conditions in the pressure chamber during the experiments, we determined the parameters of phase transitions and hydrate content characteristics in soil samples. To assess the dissociation kinetics for pore hydrates using the PVT method [6, 11, 19], we determined the parameters of hydrate saturation ( $S_h$ ) and the hydrate coefficient (the fraction of pore water converted into hydrate,  $K_h$ ) at each moment in time.

## RESULTS OF EXPERIMENTAL MODELING

The results of the experiments showed the occurrence of a self-preservation effect of methane hydrate in frozen hydrate-containing soils at a decrease in pressure below equilibrium. This effect manifests itself as a slowdown or attenuation of the dissociation rates of the pore gas hydrate. The effectiveness of self-preservation depends on several factors, such as gas pressure and temperature, dispersiveness, and the initial moisture (ice content). It was found during the experiments that a decrease in the intensity of pore hydrate dissociation in frozen rocks under pressure reduction below equilibrium in the temperature range from  $-3^\circ\text{C}$  to  $-9^\circ\text{C}$  is influenced by a sandy composition of reservoirs, increased gas pressure and ice content in the pore space, and reduced salinity [6, 11].

Additionally, it was established in [6] that methane hydrates may be preserved in a metastable state for a long time, which is typical of low-temperature ( $-4\ldots-5^\circ\text{C}$  and below) sandy and sandy–loam horizons with low salinity and high ice saturation (Fig. 3).

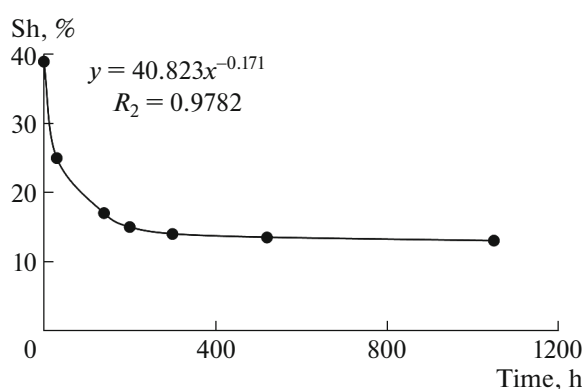


**Fig. 3.** Change in hydrate saturation ( $S_h$ ) of frozen sand in time at  $-6^\circ\text{C}$  at a decrease in gas pressure from equilibrium to 0.1 MPa.

Based on the experimental data approximation in [6] (Fig. 3), the analytical dependence of residual hydrate saturation on time was proposed:

$$S_h = At^{-n}, \quad n = 0.15\text{--}0.17, \quad A = \text{const}, \quad (20)$$

where  $\tau$  is the lifetime of self-preserving pore gas hydrate,  $n$  is a constant within 0.15–0.17, and  $A$  relates to the initial content of the pore hydrate. Equation (20) can be used to predict changes in the hydrate saturation of frozen soils in the case of self-preservation of pore hydrates. According to the predictive curve, the residual hydrate content over tens of thousands of years may be at the level of several percent, which confirms the possibility of long-term (thousands of years) existence of relic gas hydrates in the depths of frozen rocks in the northern part of Western Siberia.

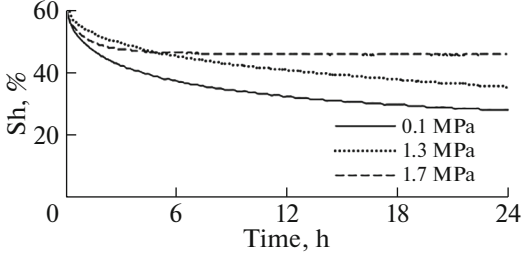
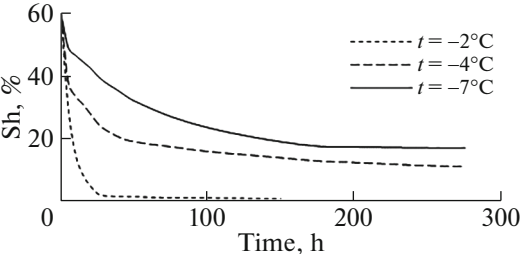
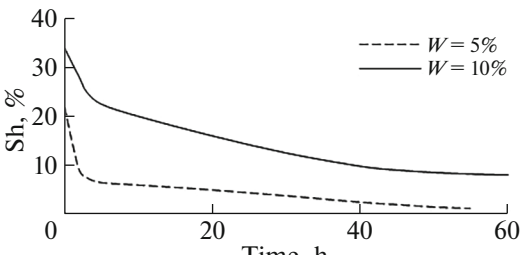
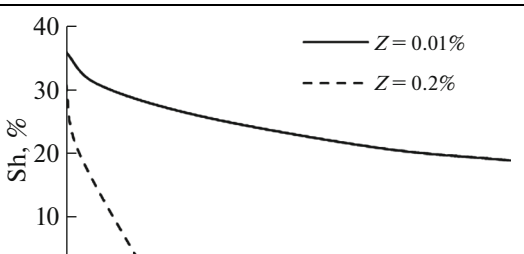
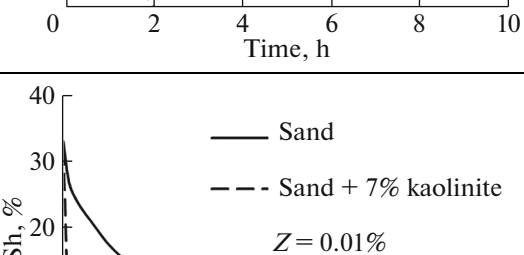
The experimental data presented by E. Chuvilin et al. [11], obtained from the results of physical modeling of methane hydrate pore dissociation and self-preservation processes in frozen sandy samples collected from gas-bearing horizons of the cryolithozone, allowed identifying the main characteristics of the geological environment that influence the intensity of self-preservation (Table 1).

## DISCUSSION

We compare the results obtained based on the proposed mathematical model derived from (19) to the results from formula (20) and Table 1 obtained from the experimental studies. Excluding variable  $\xi$  from Eq. (19) together with coefficients  $a_1$  and  $a_2$  from formulas (11), where the average pressure is determined as  $\bar{p} = (p_0 + p^0)/2$ , we obtain

$$S_h = \frac{p^0}{R_g T_0 (1 - \gamma_i) \rho_h} C_0 t^{-a_2} \operatorname{erf} \left( \frac{x}{\sqrt{2a_1 t}} \right), \quad (21)$$

**Table 1.** Main factors determining self-preservation of pore methane hydrates in frozen rocks\*

Factor	Influence	Kinetics of methane hydrate dissociation in the pore space of frozen samples after depressurization
Gas pressure	An increase in the external pressure $p^0$ increases preservation of pore hydrate	
Temperature	A decrease in the negative temperature decreases the intensity of pore hydrate dissociation	
Initial moisture (ice content)	An increase in the initial ice content decreases the intensity of pore hydrate dissociation	
Salinity	An increase in salt ions ( $Z$ ) decreases the stability of the pore hydrate	
Clay particles	An increase in the content of the clay component reduces preservation of the pore hydrate	

\* The figures are presented in accordance with [11].

$$a_1 = \frac{k_1 \bar{p} t_0}{\mu \phi l^2}, \quad a_2 = \frac{k_2 \bar{p}}{\gamma \mu \phi}, \quad \bar{p} = \frac{p_0 + p^0}{2}. \quad (22)$$

These formulas allow us to determine the local kinetics of gas hydrate decomposition. Far from the reservoir depressurization boundary, we have

$$S_h = \frac{p^0}{R_g T_0 (1 - \gamma_i) \rho_h} C_0 t^{-a_2}.$$

Near the reservoir depressurization boundary, we obtain the expression

$$S_h \approx \frac{p^0}{R_g T_0 (1 - \gamma_i) \rho_h \sqrt{2a_1}} C_0 x t^{-a_2-1/2}.$$

Hence, it follows that the hydrate decomposes faster near the depressurization boundary. By averaging (21) over a large interval (the thickness of the reservoir), we have

$$S_h = \frac{p^0}{R_g T_0 (\gamma_i - 1) \rho_h} C_0 t^{-a_2}. \quad (23)$$

Comparing (23) and (20), we obtain

$$n = a_2, \quad (24)$$

$$A = \frac{p^0}{R_g T_0 (1 - \gamma_i) \rho_h} C_0. \quad (25)$$

Here,  $C_0$  is a constant characterizing the initial gas volume in the reservoir or the sample.

Formulas (24), (25), and (22) show the dependence of the exponent of the power law of gas hydrate decomposition (20) and the coefficient of this law on the parameters of the problem. Thus, the model under consideration yields power law (23), as does experiment (20) with exponent (24) and coefficient (25).

Next, we consider the properties obtained from the experiments (Table 1), based on equations (21)–(25):

(1) *Ice content.* The increase in the ice content in this model implies the decrease in permeability  $k_1$ , i.e., the decrease in  $a_1$ . It is seen from (21)–(22) that at a decrease in  $a_1$  the residual hydrate saturation  $S_h$  at an arbitrary point  $x$  increases. This is also evident from general physical considerations, since poor gas removal from the reservoir leads to an increase in pressure within it and consequently slows down the gas hydrate decomposition.

(2) *Temperature.* As known, at a decrease in temperature, the equilibrium pressure  $p_0$  decreases, so does  $\bar{p}$  (22) and, consequently, the parameter  $a_2 = n$  decreases, meaning that the exponential function  $t^{-a_2}$  increases. Moreover, at a decrease in temperature, the coefficient in law (23) also increases. Therefore, according to (23),  $S_h$  increases at a decrease in the temperature.

(3) *Pressure.* According to (25), as the external pressure  $p^0$  increases, the parameter  $A$  increases too, and, according to (23), the residual hydrate saturation also increases.

(4) *Salinity.* Salinity is not considered in the model. However, if we take into account that the initial equilibrium pressure  $p_0$  increases with increasing salinity, and so does  $a_2$  (22), then it follows that the residual hydrate saturation decreases with increasing salinity.

Thus, under the selected parameters, we not only have qualitative but also good quantitative agreement with the experiment.

## CONCLUSIONS

The results of mathematical modeling of pore methane hydrate dissociation in frozen rocks using the model we proposed made it possible to describe the kinetics of inhibition of decomposition of the pore hydrate at a decrease in the equilibrium pressure, associated with the manifestation of the self-preservation effect, which was previously identified during experimental studies. According to the data of mathematical and physical modeling, the rate of decrease in residual hydrate saturation of frozen rocks under conditions of metastability of the pore hydrate have a power law character, which indicates the possible long-term preservation of hydrates in the pore space of frozen rocks at pressures below equilibrium.

Due to the results of mathematical modeling, we proposed a more general (compared to power law) kinetics law for the decomposition of the pore gas hydrate, which takes into account gas filtration in the reservoir, as well as its depressurization through the upper boundary. In addition, based on the mathematical investigation, an explicit dependence was established between the coefficient of the power law  $A$  and its exponent  $n$  on the problem parameters  $a_1$  and  $a_2$ , determined by the properties of the reservoir, the gas hydrate, and the ice film covering the gas hydrate. The obtained dependences on the kinetics of pore hydrate dissociation in frozen rocks not only confirm the influence of natural environmental factors obtained experimentally but also explain them.

## FUNDING

This work was supported by the Russian Science Foundation (grant nos. 22-67-00025, 21-77-10074, and 22-17-00112). We are grateful to Ministry of Science and Higher Education of the Russian Federation for the support provided to Tomsk State University under the project “Priority-2030.”



# ETHICS APPROVAL AND CONSENT TO PARTICIPATE

This work does not contain any studies involving human and animal subjects.

# CONFLICT OF INTEREST

The authors of this work declare that they have no conflicts of interest.

# REFERENCES

1. V. A. Istomin and V. S. Yakushev, *Gas Hydrates under Natural Conditions* (Nedra, Moscow, 1992) [in Russian].
2. N. N. Romanovskii, *Fundamentals of Cryogenesis in the Lithosphere* (Moscow State Univ., Moscow, 1993) [in Russian].
3. E. M. Chuvilin, V. S. Yakushev, and E. V. Perlova, *Polarforschung* **68**, 215–219 (2000).
4. A. A. Trofimuk, Yu. F. Makogon, and V. S. Yakushev, *Sov. Geol. Geofiz.* **27** (11), 3–10 (1986).
5. V. S. Yakushev, *Natural Gas and Gas Hydrates in Cryolithozone* (LLC VNIIGAZ, Moscow, 2009) [in Russian].
6. E. Chuvilin, B. Bukhanov, D. Davletshina, S. Grebenkin, and V. Istomin, *Geosciences* **8** (12), 431:1–431:12 (2018).
7. E. D. Ershov, Yu. P. Lebedenko, E. M. Chuvilin, V. A. Istomin, and V. S. Yakushev, *Dokl. Akad. Nauk* **321** (4), 788–791 (1991).
8. V. S. Yakushev, E. V. Perlova, N. A. Makhonina, E. M. Chuvilin, and E. V. Kozlova, *Russ. Khim. Zh.*, No. 3, 80–90 (2003).
9. A. Hachikubo, S. Takeya, E. Chuvilin, and V. Istomin, *Phys. Chem. Chem. Phys.* **13**, 17449–17452 (2011).
10. L. S. Podenko, A. O. Drachuk, N. S. Molokotina, and A. N. Nesterov, *Zh. Fiz. Khim.* **92** (2), 239–246 (2018).
11. E. Chuvilin, D. Davletshina, B. Bukhanov, A. Mukhametdinova, and V. Istomin, *Geosciences* **12** (11) (2022).  
<https://doi.org/10.3390/geosciences12110419>
12. H. Mimachi, S. Takeya, A. Yoneyama, K. Hyodo, T. Takeda, Y. Gotoh, and T. Murayama, *Chem. Eng. Sci.* **118**, 208–213 (2014).
13. S. Y. Misyura and I. G. Donskoy, *Chem. Eng. Sci.* **148**, 65–77 (2016).
14. G. I. Barenblatt, L. I. Lobkovsky, and R. I. Nigmatulin, *Dokl. Earth Sci.* **470** (2), 1046–1050 (2016).
15. M. M. Ramazanov and L. I. Lobkovskii, *Fluid Dyn.* **53** (4), 517–531 (2018).
16. L. I. Lobkovskii and M. M. Ramazanov, *Dokl. Earth Sci.* **484** (1), 105–109 (2019).
17. V. A. Vlasov, *Inzh.-Fiz. Zh.* **92** (6), 2449–2457 (2019).
18. L. I. Lobkovsky, M. M. Ramazanov, I. P. Semiletov, and D. A. Alekseev, *Geosciences* **12** (9), 345 (2022).  
<https://doi.org/10.3390/geosciences12090345>
19. E. M. Chuvilin, D. A. Davletshina, and M. V. Lupachik, *Earth's Cryosphere* **23** (2), 44–52 (2019).  
<https://doi.org/10.21782/EC2541-9994-2019-2>
20. N. Shakhova, I. Semiletov, V. Sergienko, L. Lobkovsky, V. Yusupov, A. Salyuk, A. Salomatin, D. Chernykh, D. Kosmach, G. Panteleev, D. Nicolsky, V. Samarkin, S. Joye, A. Charkin, O. Dudarev, A. Meluzov, and O. Gustafsson, *Philos. Trans. A Math. Phys. Eng. Sci.* **373** (2052) (2015).  
<https://doi.org/10.1098/rsta.2014.0451>

Translated by L. Mukhortova

**Publisher's Note.** Pleiades Publishing remains neutral with regard to jurisdictional claims in published maps and institutional affiliations.